

Antitumor Activity of Lankacidin Group Antibiotics Is Due to Microtubule Stabilization via a Paclitaxel-like Mechanism

Ahmed Taha Ayoub,^{*,†,∇} Rabab M. Abou El-Magd,^{‡,○} Jack Xiao,[§] Cody Wayne Lewis,^{‡,◆} Tatiana Martins Tilli,^{||} Kenji Arakawa,[⊥] Yoshi Nindita,[⊥] Gordon Chan,^{‡,◆} Luxin Sun,[#] Mark Glover,[#] Mariusz Klobukowski,[†] and Jack Tuszynski[‡]

[†]Department of Chemistry, University of Alberta, Edmonton, AB, T6G 2G2, Canada

[‡]Department of Oncology, Cross Cancer Institute, University of Alberta, Edmonton, AB, T6G 1Z2, Canada

[§]Department of Electrical and Computer Engineering, University of Alberta, Edmonton, AB, T6G 1H9, Canada

^{||}National Institute of Science and Technology for Innovation in Neglected Diseases, Rio de Janeiro, 21040-361 Brazil

[⊥]Department of Molecular Biotechnology, Graduate School of Advanced Sciences of Matter, Hiroshima University, Hiroshima 739-8530, Japan

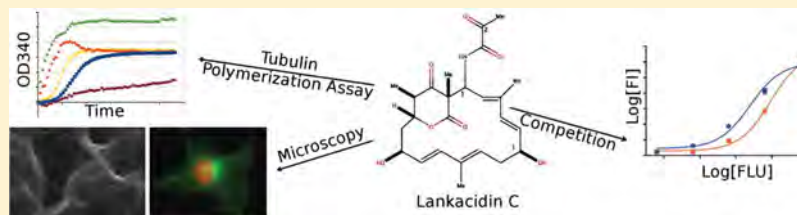
[#]Department of Biochemistry, University of Alberta, Edmonton, AB, T6G 2H7, Canada

[∇]Medicinal Chemistry Department, Heliopolis University, Cairo 11777, Egypt

[○]City for Scientific Research and Technology Applications, Alexandria, 21934 Egypt

[◆]Cancer Research Institute of Northern Alberta, University of Alberta, Edmonton, AB, T6G 2J7, Canada

S Supporting Information



ABSTRACT: Lankacidin group antibiotics show strong antimicrobial activity against various Gram-positive bacteria. In addition, they were shown to have considerable antitumor activity against certain cell line models. For decades, the antitumor activity of lankacidin was associated with the mechanism of its antimicrobial action, which is interference with peptide bond formation during protein synthesis. This, however, was never confirmed experimentally. Due to significant similarity to paclitaxel-like hits in a previous computational virtual screening study, we suggested that the cytotoxic effect of lankacidin is due to a paclitaxel-like action. In this study, we tested this hypothesis computationally and experimentally and confirmed that lankacidin is a microtubule stabilizer that enhances tubulin assembly and displaces taxoids from their binding site. This study serves as a starting point for optimization of lankacidin derivatives for better antitumor activities. It also highlights the power of computational predictions and their aid in guiding experiments and formulating rigorous hypotheses.

■ INTRODUCTION

Lankacidin-group antibiotics (T-2636) are fermentation products that are produced by the organism *Streptomyces rochei*.¹ First isolated in 1969, the antibiotic group was later fully characterized and the structure of lankacidin was elucidated.^{2–5} The parent of this group, lankacidin C (Figure 1a), is a 17-membered macrocyclic tetraene that shows strong antimicrobial activity against various Gram-positive bacteria, including many strains that are resistant to macrolide antibiotics, and is used in veterinary medicine.⁶

Besides its antimicrobial activity, lankacidin C and some of its derivatives also displayed considerable in vivo antitumor activity against several models such as L1210 leukemia, B16 melanoma, and 6C3 HED/OG lymphosarcoma.^{8,9} In addition to its pharmacological activities, the drug also has a complete

synthetic pathway available¹⁰ that makes it attractive for optimization.

The antimicrobial mechanism of action of lankacidin has been attributed to interference with peptide bond formation during protein synthesis by binding at the peptidyl transferase center of the eubacterial large ribosomal subunit.^{11,12} It is unclear, however, whether the antitumor activity of lankacidins is related to their interference with protein synthesis or not.⁹ Hence, the mechanism of antitumor activity of lankacidins is yet to be elucidated.

In a previous virtual screening study for paclitaxel-like microtubule stabilizers, we have identified a novel scaffold,

Received: August 22, 2016

Published: October 8, 2016

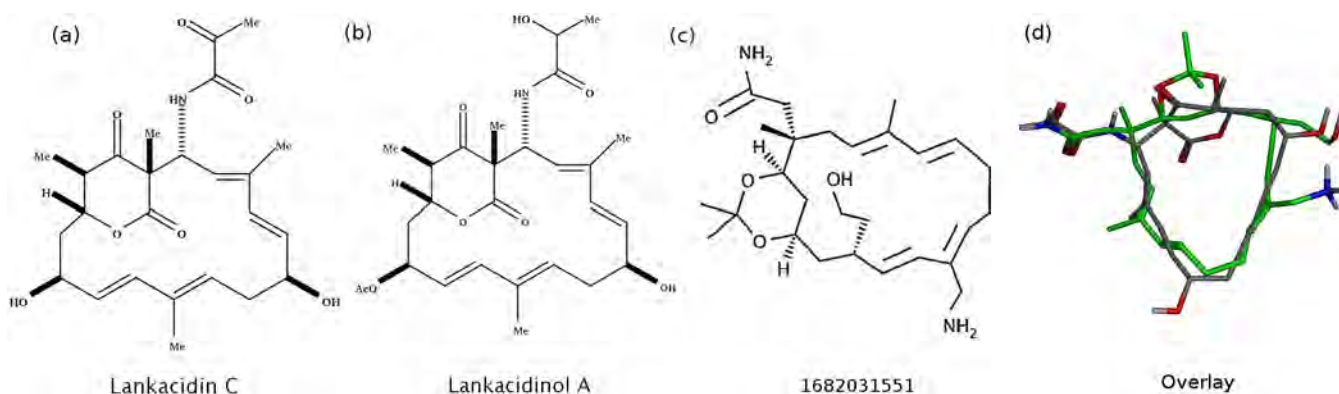


Figure 1. Structures of lankacidin C (a), lankacidinol A (b), virtual screening hit 1682031551⁷ (c), and a 3D overlay of lankacidin C (gray) with molecule 1682031551 (green) (d).

molecule 1682031551 in Figure 1c and others, predicted to bind to tubulin at the paclitaxel binding site.⁷ Faced with the difficulty of synthesizing these novel compounds, we tried using 2D molecular fingerprints to search for available molecular structures that resemble them. It turned out that the molecular framework of our novel hits very closely resembles that of lankacidin; see Figure 1d. The striking similarity between the two compounds suggests a hypothesis that lankacidin C, and its group, could also bind to tubulin at the paclitaxel binding site which could explain its unknown antitumor mechanism of action. In addition to explaining their mechanism of action, if this hypothesis is tested and proven true, this would widen our understanding of microtubule stabilization by paclitaxel-like agents and would also open the door for structural modifications of lankacidins toward better binding with tubulin. This may help provide a promising cancer treatment. On the computational side, if the theory is proven right, this would provide a good example of the power of computational predictions and their aid in explaining chemical and pharmacological processes. In the current work, we use computational simulations, cell-based assays, and microtubule polymerization assays together with imaging through microscopy to test the hypothesized mechanism of antitumor action of lankacidin group antibiotics.

RESULTS AND DISCUSSION

Computational Simulations. In order to estimate the binding energy between lankacidin C and tubulin, molecular dynamics simulations of the complex of lankacidin C bound at the paclitaxel-binding site of β -tubulin was performed. The last 5 ns of the 11 ns trajectory were postprocessed by removal of water and ions, and MM/PBSA (molecular mechanics/Poisson–Boltzmann surface area) and normal-mode analyses were run. MM/PBSA returned a binding energy of -34.5 kcal/mol, while normal-mode analysis returned an entropic contribution ($T\Delta S$) of -23.4 kcal/mol. Both values yield a calculated binding free energy of -11.1 kcal/mol. By utilization of the linear fitting that was developed in previous work,⁷ this value can be extrapolated using the following relationship,

$$\Delta G_{\text{predicted}} = 0.2 \Delta G_{\text{calculated}} - 4.7 \quad (1)$$

to give the predicted binding energy of lankacidin C to the paclitaxel binding site. The equation yields a predicted binding energy of -7.4 ± 0.9 kcal/mol. When this value is compared to known paclitaxel-like microtubule stabilizers upon which the linear fit was built, it is closest to sarcodictyin A which has a

predicted binding energy of -8.6 ± 0.7 kcal/mol.⁷ Since it is established in previous studies that the antitumor activity of lankacidin C is relatively weak,^{8,9} the comparison of our predicted binding energy of lankacidin C to the paclitaxel binding site versus that of the relatively weak sarcodictyin A seems plausible. Hence, our computational calculations predict that lankacidin C could be performing its antitumor activity via interference with microtubule growth through binding at the paclitaxel binding site.

Lankacidin is a Cytotoxic Microtubule Stabilizing Agent. Cell Viability Assay. Antitumor activity of lankacidin-group antibiotics against several cell line models was already established more than 4 decades ago.^{8,9} The activity of lankacidin C against the HeLa cell line model, however, was almost null, contrary to some of its derivatives that showed considerable activity. In the current work, we retested lankacidin C against the HeLa cell line. We also tested the drug against the breast cancer T47D cell line on which, to our knowledge, the drug has never been tested. Figure 2 shows the different cell viability curves as well as the IC_{50} values after 48, 72, and 96 h of incubation in the presence of the drug. As expected, HeLa cell lines have very little sensitivity to lankacidin C with an IC_{50} of $223.5 \mu\text{M}$ after 96 h. The T47D breast cancer cell line, however, is about 20-fold more sensitive to lankacidin C with an IC_{50} of $11.1 \mu\text{M}$ after 96 h.

Cell Imaging Assay. To examine the effect of lankacidin C on microtubules in cells, T47D cells were treated with 1 mM lankacidin C. Paclitaxel and colchicine were used as controls: paclitaxel at 100 nM concentration as a control for microtubule stabilizing agents and colchicine at $0.5 \mu\text{M}$ concentration as a control for microtubule destabilizing agents. The reason why we used such very high concentrations in these experiments is because the effect of some microtubule interacting drugs on microtubule bundling only starts to be visible in cells under the microscope when the concentration of the drugs is higher than 31 times its IC_{50} value.¹³ The effect becomes more visible with even higher concentrations of the drugs.

The results are shown in Figure 3. In normal cells, microtubules are less dense and mitotic cells appear normal. In concichicine-treated cells, microtubules are broken down and appear as small dots in the cytoplasm. On the other hand, paclitaxel treatment, as expected, resulted in a dense microtubule network. Microtubule bundles could also be seen in interphase cells, while hallmark multipolar disrupted spindles are visible in mitotic cells. Lankacidin C treatment also resulted in dense microtubules in interphase cells and disrupted spindles

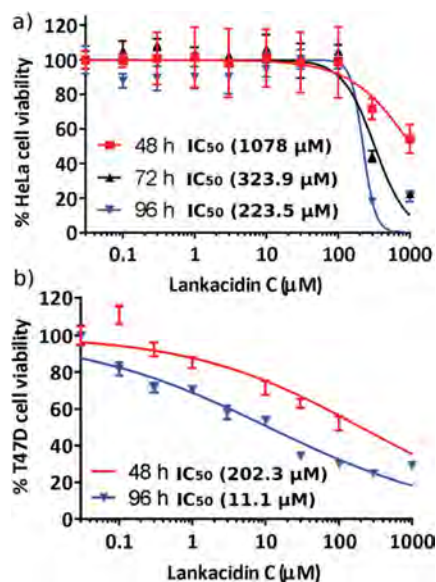


Figure 2. Lankacidin C reduces cell viability in human cancer cell lines. HeLa (a) and T47D cells (b) were treated in triplicate with increasing concentrations of lankacidin C for 48 h, 72 h to 96 h, and cell viability was measured. IC_{50} values are included in the figure. Experiments were repeated twice, and the mean values and standard error of mean are shown.

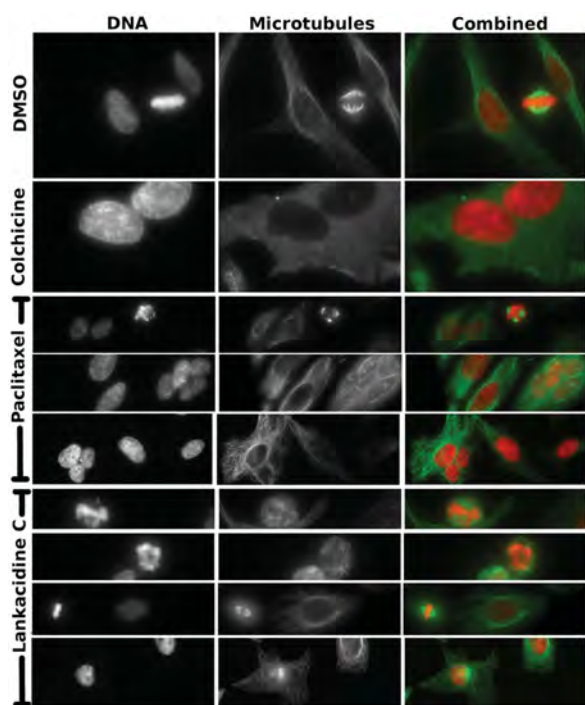


Figure 3. Lankacidin C disrupts microtubules in T47D cells. T47D cells were treated with DMSO as a negative control, 0.5 μ M colchicine, 100 nM paclitaxel, or 1 mM lankacidin C for 2 h. Immunofluorescence was performed with anti-tubulin antibodies (green), and DNA was stained with DAPI (4',6-diamidino-2-phenylindole, red).

in mitotic cells, a phenotype that is more similar to paclitaxel-treated cells than colchicine-treated cells. It should be noted that despite the high concentration of lankacidin that we used, a more pronounced visual effect would still require even higher concentrations as proven earlier.¹³ This was, however, not possible due to solubility limitations.

Tubulin Polymerization Assay. It was demonstrated in the 1970s that microtubule solutions scatter light in a concentration-dependent manner.^{14,15} Upon the basis of an adaptation of this concept, the tubulin polymerization assay (Cytoskeleton, Inc., catalog no. BK006P) was built. The growth of microtubules, at different conditions and in the presence of different agents, is followed by recording the optical density of the solution at a wavelength of 340 nm for a period of time, and a curve is plotted.

Figure 4 shows the polymerization curves at different conditions. In the absence of any agents, the curve has three

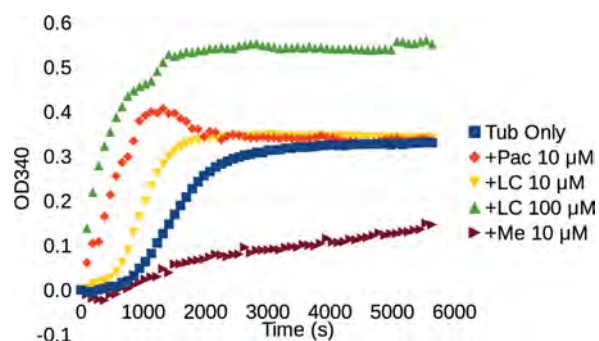


Figure 4. Tubulin polymerization curves at different conditions. Polymerization is followed by plotting the optical density at 340 nm versus time. The plots show polymerization in the absence of any agent, in the presence of 10 μ M paclitaxel (Pac), 10 μ M lankacidin C (LC), 100 μ M lankacidin C, or 10 μ M mebendazole (Me).

distinctive phases: a nucleation phase where no growth occurs, growth phase where maximum growth rate occurs, and a steady state phase where the concentration of polymerized tubulin remains constant. In the absence of any agent, a long nucleation phase of about 10 min occurs followed by a maximum growth rate (V_{max}) of 13 mOD/min. The steady state phase occurs at an OD340 (optical density at 340 nm) of nearly 0.33. In the presence of 10 μ M of the microtubule stabilizer paclitaxel, the nucleation phase is totally bypassed and a fast growth at V_{max} of 21 mOD/min occurs. The plateau level is a bit higher indicating a slightly higher final polymer mass. In the presence of 10 μ M microtubule destabilizer mebendazole, the nucleation phase is slightly lengthened and V_{max} declines to 4 mOD/min. The final polymer mass also reduces to half of its normal value. These results confirm the utility of this assay in indicating the effect of a drug on the stability and polymerization of microtubules as well as possible cytotoxic effects.

In the presence of 10 μ M of lankacidin C, the nucleation phase is shortened and growth is enhanced through a V_{max} of 18 mOD/min. The final polymer mass is slightly increased. In the presence of 100 μ M lankacidin C, the nucleation phase is totally bypassed and a very fast growth phase with a V_{max} of 35 mOD/min follows. The final polymer mass is almost doubled. The polymerization assay thus proves that lankacidin C is a microtubule stabilizing agent that enhances microtubule growth. It also indicates that the antitumor activity of lankacidin C is likely due to interference with microtubule growth by stabilization.

Microtubule Imaging. In order to verify that the structures formed in the presence of lankacidin C are actually microtubules, we carried out another polymerization assay. In this assay, however, rhodamine labeled tubulin dimers were used in the polymerization to aid in viewing microtubules after

polymerization. In Figure 5, the morphologies of the negative control (untreated microtubules), colchicine-treated micro-

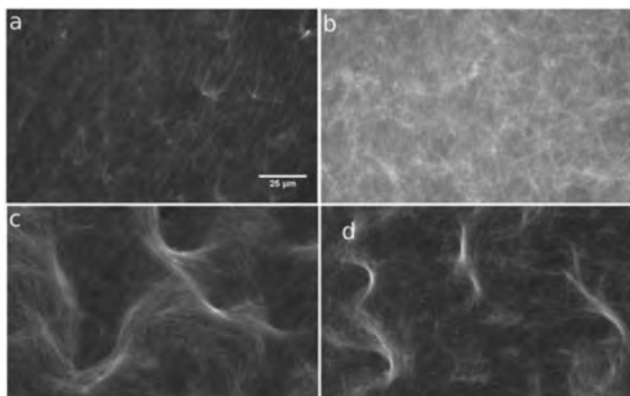


Figure 5. Morphology of microtubules following drug treatment: (a) negative control (tubulin only), (b) colchicine-treated (10 μM), (c) lankacidin C-treated (10 μM), (d) paclitaxel-treated (10 μM). The morphology of lankacidin-treated microtubules appears very similar under the microscope to that of paclitaxel-treated microtubules.

tubules, lankacidin C-treated microtubules, and paclitaxel-treated microtubules, all drugs at a concentration of 10 μM , are presented.

In the absence of any drugs (Figure 5a), tubulin dimers polymerized into short strands of microtubules diffused throughout. In the presence of colchicine (Figure 5b), tubulin dimers polymerized into short strands of microtubules with an increased background fluorescence indicating the abundance of unpolymerized tubulin dimers in the solution. Paclitaxel-treated tubulin dimers (Figure 5d) polymerized into long strands of microtubules which aggregate together forming bundles of microtubules. Microtubules polymerizing in the presence of lankacidin C (Figure 5c) also display longer strands that aggregate into microtubule bundles, in an effect that is similar to paclitaxel. This experiment shows that the structures produced in the presence of lankacidin C are actually microtubules, and it also confirms that the effect of lankacidin C on microtubules is similar to paclitaxel, confirming our hypothesis.

Lankacidin Binds Microtubules at the Paclitaxel Binding Site. To test the binding of lankacidin to the paclitaxel binding site, a relatively high concentration of assembled tubulin (microtubules) was required. Therefore, another polymerization assay was done using a higher concentration of tubulin (10 mg/mL) at 7.8% glycerol concentration as described in the methods section. After an hour of incubation at 37 $^{\circ}\text{C}$ and measurement of the optical density, the curve in Figure 6 was obtained.

Due to the very high concentration of tubulin used, the nucleation phase is bypassed and growth is very fast as the figure shows. In addition, the length of the steady state phase confirms the stability of microtubules as long as they are kept in the right buffer (80 mM PIPES, pH 6.9, 2 mM MgCl_2 , 0.5 mM EGTA (ethylene glycol-bis(β -aminoethyl ether)- N,N,N',N' -tetraacetic acid), 7.8% glycerol, 1 mM GTP) and at the right temperature (37 $^{\circ}\text{C}$). Hence, we made sure that all the competitive binding assays are done at the right buffer and temperature conditions to preserve microtubule stability. According to the manufacturer's specifications, every 0.1 increase in optical density reflects an increase in the

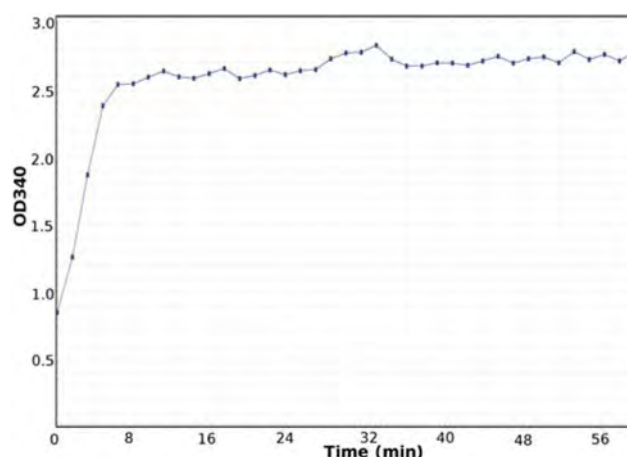


Figure 6. Tubulin polymerization curve for preparing microtubules for competitive binding assays. Data are not blank corrected.

concentration of assembled tubulin of nearly 10 μM . Therefore, Figure 6 shows that the concentration of assembled tubulin in our microtubule sample is nearly 150 μM . As described in the methods section, this microtubule was used in the flutax-2 competitive binding assay.

The binding of increasing concentrations of the fluorescent taxoid flutax-2 to microtubules was tested in the presence and absence of 128 μM of lankacidin C, and the curves in Figure 7

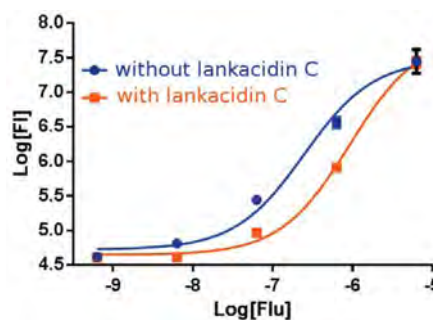


Figure 7. Competitive binding assay: a plot of the logarithm of the fluorescence intensity ($\log[\text{F}]$) of flutax-2 bound to microtubules versus the initial concentration of flutax-2 in the sample ($\log[\text{Flu}]$), in the presence or absence of lankacidin C.

were obtained. The curve plots the logarithm of the fluorescence intensity of flutax-2 pelleted after centrifugation (i.e., flutax-2 bound to microtubules) versus the logarithm of the initial concentration of flutax-2 in the sample.

The curves clearly show that the binding of flutax-2 to microtubules is inhibited in the presence of lankacidin C in a manner that reflects competitive inhibition. From the curves, the value of the EC_{50} of flutax-2 in the absence of lankacidin C was estimated to be 248 ± 50 nM, and $\text{EC}_{50}^{\text{app}}$ of flutax-2 in the presence of lankacidin C was estimated to be 921 ± 90 nM. From Michaelis–Menten kinetics, the following equation holds for competitive inhibitors,

$$K_d^{\text{app}} = K_d(1 + [\text{I}]/K_i) \quad (2)$$

where K_i is the dissociation constant of the inhibitor, lankacidin C, and $[\text{I}]$ is its concentration. From the above equation, the dissociation constant of lankacidin C from the paclitaxel binding site was estimated to be 50 ± 13 μM . This value,

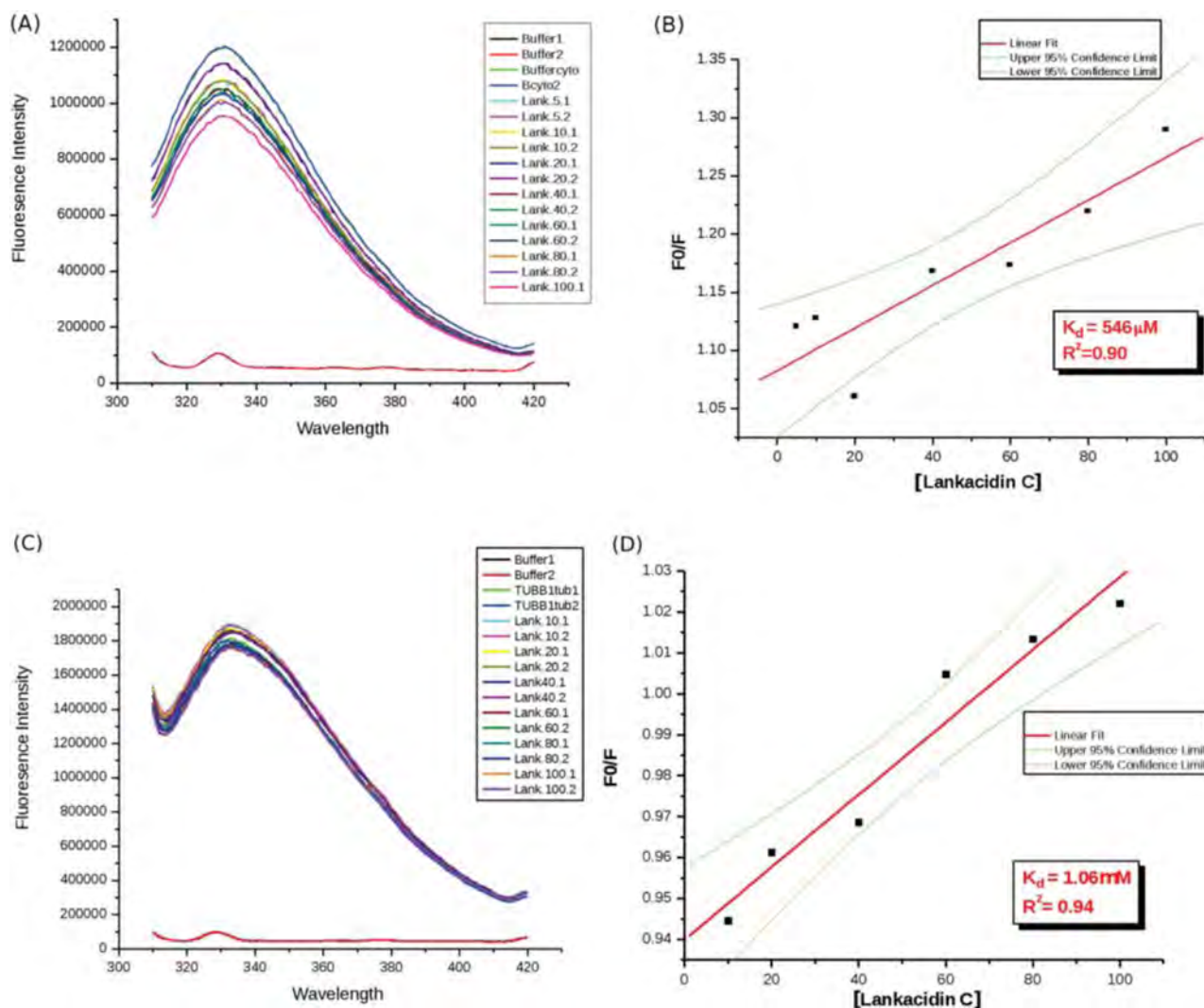


Figure 8. Fluorescence quenching of 2 μM porcine cytoskeleton tubulin (A, B) or recombinant human tubulin $\alpha I-\beta I$ (C, D) in complex with lankacidin C at different concentrations (5, 10, 20, 40, 60, 80, 100 μM).

however, only indicates that lankacidin C has an affinity to the paclitaxel binding site. It does not necessarily correlate with the potency of the drug as a cytotoxic agent. This was demonstrated by Buey et al., who showed that there is a very poor correlation ($r^2 = 0.27$) between the cytotoxicity of paclitaxel-like drugs and their affinity to the paclitaxel binding site.¹⁶

Binding to Free Tubulin. Fluorescence quenching assays were performed on lankacidin C and one of its analogues known as lankacidinol A (see Figure 1b) with free tubulin to detect if there is any binding to free tubulin dimers.

When tested against porcine cytoskeleton tubulin, the fluorescence quenching plots for lankacidin C in Figure 8A,B and for lankacidinol A in Figure 9A,B were obtained. The curves show a concentration-dependent fluorescence-quenching due to conformational changes upon the addition of lankacidin. This indicates weaker but significant binding to free tubulin with K_d values of 546 μM and 1.1 mM for lankacidin C and lankacidinol A, respectively. The curves in Figure 8C,D and Figure 9C,D show the fluorescence quenching assay against recombinant human tubulin $\alpha I-\beta I$. Similarly, both molecules induce a concentration-dependent conformational change. The characteristic tubulin fluorescence emission spectrum was

significantly quenched by lankacidinol A with a K_d value of 654 μM versus 1.06 mM for lankacidin C. The fluorescence quenching assays thus indicate that lankacidin has an affinity toward free tubulin that is significantly lower than its affinity toward assembled tubulin.

CONCLUSION

This study represents a mechanistic investigation into the cytotoxic action of lankacidin group antibiotics. Having been shown to have considerable *in vivo* antitumor activities against certain cancer cell line models, the mechanism of cytotoxicity of this group of drugs remained elusive for decades. Speculations about the cytotoxicity being linked to interference with protein synthesis, the main mechanism for antibiotic activity, have been the only explanation to date.

Due to similarity with paclitaxel-like hits from previous computational virtual screening studies, it was suggested that lankacidin could have a paclitaxel-like mechanism of cytotoxicity. In this study we have computationally and experimentally investigated this hypothesis. Computational predictions showed that lankacidin has a reasonable affinity toward paclitaxel binding sites of β -tubulin with a binding free energy of -7.4 ± 0.9 kcal/mol. Cell-based assays have confirmed that lankacidin

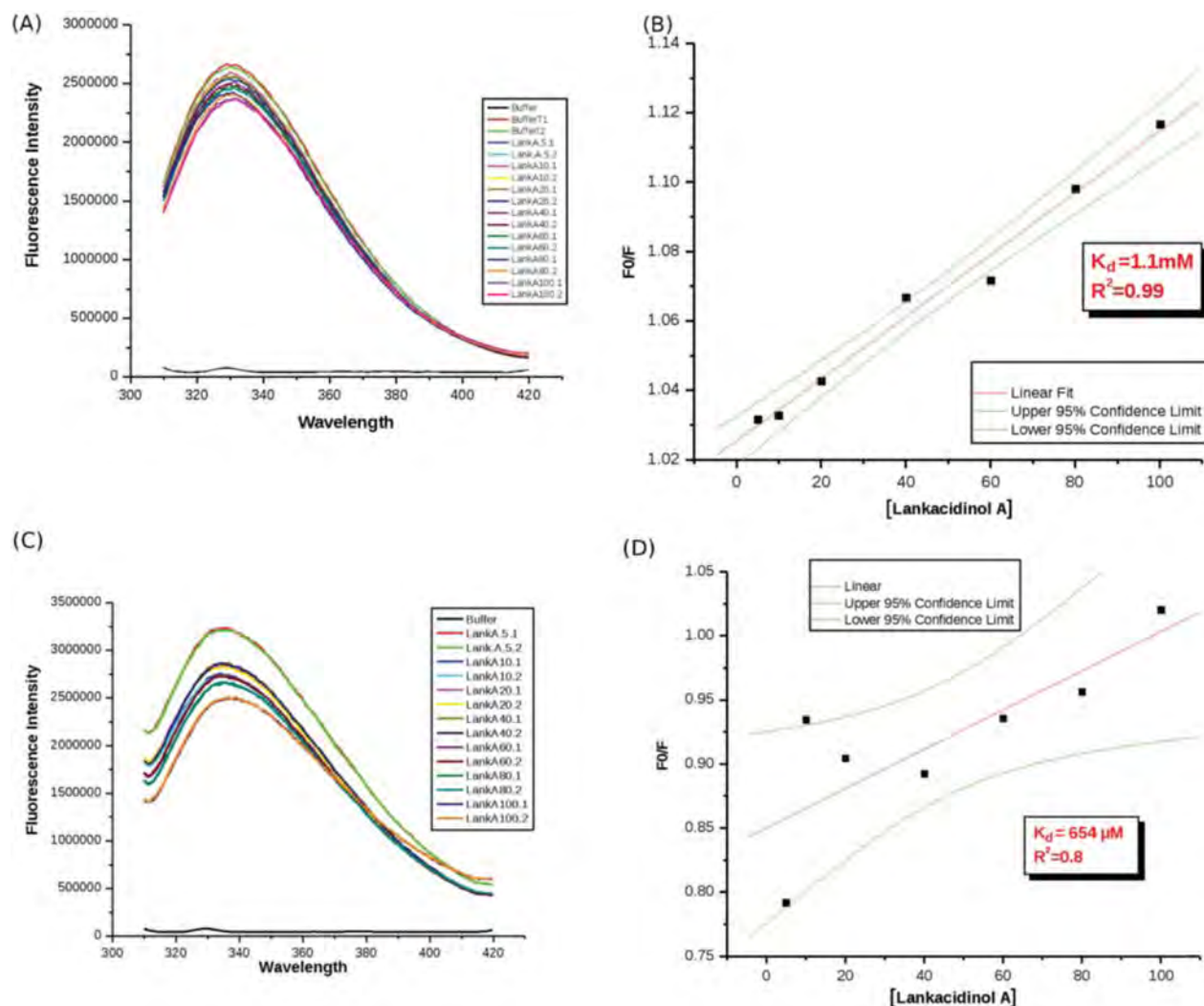


Figure 9. Fluorescence quenching of 2 μM porcine cytoskeleton tubulin (A, B) or recombinant human tubulin $\alpha\text{I}-\beta\text{I}$ (C, D) in complex with lankacidinol A at different concentrations (5, 10, 20, 40, 60, 80, 100 μM).

increases the density of microtubules in interphase cells and disrupts spindles in mitotic cells, a phenotype that is similar to the one produced via paclitaxel. Tubulin polymerization assays showed that lankacidinol antibiotic increases the rate of tubulin assembly as well as the final mass of the microtubule polymer. Imaging of the samples confirmed that the formed structures were indeed microtubules that bundle in a manner similar to the bundling of paclitaxel-treated microtubules.

Competitive binding assays showed that lankacidinol competes with fluorescent taxoid, flutax-2, for the paclitaxel binding site. A dissociation constant of $50 \pm 13 \mu\text{M}$ for lankacidinol C with the paclitaxel binding site was obtained. Fluorescence quenching assays were also performed to detect if there was any binding to free tubulin, and the results were positive. However, the affinity of lankacidinol antibiotics to free tubulin dimers is significantly less than the affinity toward assembled tubulin. The overall outcome of the study confirms the hypothesis that the cytotoxic activity of lankacidinol group antibiotics is likely to be associated with a paclitaxel-like mechanism of action through binding at the paclitaxel binding site and enhancing tubulin assembly. The results, however, do not rule out the possibility of other cellular targets or mechanisms through which cytotoxicity could be taking place.

The results should serve as a starting point for optimization of this class of molecules for higher affinity and better toxicological profile.

EXPERIMENTAL SECTION

Computational Simulations. Computational simulations of lankacidinol C bound to the paclitaxel binding site in β -tubulin were carried out according to the procedures outlined in previous work.⁷ Briefly, we parametrized GDP-bound β -tubulin subunit using AMBER ff99SB force field for the protein¹⁷ and Meagher et al. parameter set for GDP molecule.¹⁸ Lankacidinol C was parametrized using the GAFF force field.¹⁹ Prior to molecular dynamics simulations, the crystal structure of lankacidinol C from PDB code 3JQ4 was docked to the paclitaxel binding site using AutoDock 4.2 as explained in previous work.⁷ The complex was then neutralized, solvated, heated to 300 K, and taken through a molecular dynamics simulation for density equilibration followed by a production phase for nearly 11 ns using the AMBER package.²⁰ 500 evenly spaced snapshots from the last 5 ns of the simulation were used for an MM/PBSA binding energy calculation in which both enthalpy and entropy were estimated, the latter using normal-mode analysis. Using a linear fitting that was developed previously,⁷ we extrapolated the MM/PBSA-calculated binding energy to get a more realistic value that could be compared to binding energies of available microtubule stabilizers.

Isolation of Lankacidin. *Streptomyces rochei* strain 51252²¹ was cultured in YM liquid medium (0.4% yeast extract, 1.0% malt extract, and 0.4% D-glucose, pH 7.3) at 28 °C for 2 days. The culture broth was extracted twice with equal volume of ethyl acetate. The combined organic phase was dried (Na₂SO₄), filtered, and concentrated to dryness. The crude residue was purified by Sephadex LH20 (GE Healthcare) with methanol. The fractions containing lankacidin C and lankacidinol A were combined and further purified by silica gel chromatography with a mixture of chloroform–methanol (50:1 to 20:1). ¹H NMR spectra were measured and were identical to the reported data (see Supporting Information).²² Purity was determined using HPLC (details and chromatograms can be found in Supporting Information). The purities of lankacidin C and lankacidinol A obtained were 96.0% and 95.5%, respectively.

Cell-Based Assays. Cell Culture and Synchronization. HeLa cells were grown as a monolayer in high-glucose DMEM (Dulbecco's modified Eagle medium) supplemented with 2 mM L-glutamine and 10% (v/v) FBS (fetal bovine serum). T47D cells were grown in RPMI1640 supplemented with 2 mM L-glutamine, 10% (v/v) FBS, 0.01 mg/mL insulin, and 1 mM sodium pyruvate. Cells were grown in a humidified incubator at 37 °C with 5% CO₂.

Cell Viability Assay. In all of the following assays, the drugs were dissolved in DMSO and the concentrations of DMSO were equivalent across each of the drug treatment groups. Cells were plated into a 96-well plate at a density of 2000 cells/well for 24 h prior to treatment. Cells were then treated in triplicate with increasing concentrations of lankacidin C for the indicated treatment times (48–96 h). After treatment, cell viability was analyzed as specified in the CellTiter-Blue cell viability assay (Promega) protocol. An amount of 10 μL of CellTiter-Blue reagent was added to each well for 2–4 h. Fluorescence intensity of each well was then determined by Optima Microplate reader (560ex/590em).

Fluorescence Microscopy. Cells were processed for immunofluorescence as previously described.²³ Cells were seeded onto coverslips at a density of 5 × 10⁴ cells/mL in a 35 mm dish. Following cell synchronization cells were treated with the following inhibitors: 1% DMSO (solvent control), 100 nM paclitaxel, 0.5 μM colchicine, or 1 mM lankacidin C for 2 h. DNA was stained with 0.1 μg/mL DAPI. Coverslips were stained with anti-tubulin antibodies (Sigma; T5168; 1:4000 dilution) and Alexa Fluor 488 conjugated anti-mouse (1:1000 dilution; Molecular Probes). A microscope (Imager.Z.1; Carl Zeiss) equipped with epifluorescence optics was used to collect the images. Cells were visualized with a 63X Plan-Apochromat objective (Carl Zeiss) with 1.4 NA. Images were captured with a SensiCam (Cooke) charge-coupled device camera (PCOTECH, Inc.) controlled by Metamorph 7.0 software (Universal Imaging Corp.). Images were processed using Photoshop CC (Adobe). Coverslips were mounted with 1 mg/mL Mowiol 4-88 (EMD Millipore) in phosphate buffer, pH 7.4.

Microtubule-Based Assays. Tubulin Polymerization Assay. The tubulin polymerization assay kit was purchased from Cytoskeleton, Inc. (catalog no. BK006P). The assay was performed following the instructions in the supplied manual. To summarize, a 96-well microtiter plate was prewarmed to 37 °C for 30 min. In this plate, 10 μL of paclitaxel solution, lankacidin solutions, mebendazole solution, or a buffer solution (as a negative control) was added to 100 μL of tubulin in a buffer. This resulted in five samples having final concentrations of 10 μM paclitaxel, 10 μM lankacidin C, 100 μM lankacidin C, 10 μM Mebendazole, or a negative control, all dissolved in a solution containing final concentrations of 3 mg/mL tubulin, 80 mM PIPES, pH 6.9, 2 mM MgCl₂, 0.5 mM EGTA, 7.8% glycerol, and 1 mM GTP. The plate was immediately placed in a 37 °C prewarmed BMG FLUOstar Omega microplate reader to follow microtubule growth through optical density. The optical density at 340 nm (OD340) and 37 °C was recorded every 94 s using medium orbital shaking for 61 cycles. The experiment was repeated three times for all samples except for the mebendazole sample where only two trials were done. The average curve of OD340 versus time was plotted, and parameters were studied.

Microtubule Imaging. Rhodamine labeled tubulin dimers and unlabeled tubulin were purchased from Cytoskeleton, Inc. Following reconstitution, one part labeled tubulin was diluted in 4 parts unlabeled tubulin to give 5 mg/mL tubulin dimers in G-PEM buffer (12% glycerol, 80 mM PIPES, 1.8 mM MgCl₂, 0.6 mM EGTA, 1 mM GTP, pH 7.0). Tubulin dimers were polymerized in accordance with Cytoskeleton, Inc.'s "Tubulin Protein Datasheet Applications: In Vitro Polymerization for Fluorescent Microtubules". Tubulin dimers (4 μL) were incubated at 37 °C for 20 min to form microtubules. To each aliquot, 1 μL of lankacidin C, colchicine, paclitaxel, or buffer solution was added to produce microtubules treated with 10 μM lankacidin C, 10 μM colchicine, 10 μM paclitaxel, or negative control. Microtubule solutions were incubated at 37 °C for another 5 min in the presence of drug of interest. Following polymerization and drug treatment, microtubules were immediately imaged. Microtubules solutions were diluted in their respective prewarmed buffers to yield a final concentration of 1.3 mg/mL of tubulin dimers. Fluorescence imaging was performed on an upright microscope (Imager.Z.1, Carl Zeiss, Inc.) with 40× oil immersion objective lens (numerical aperture 1.4). All images were acquired by SensiCam charged coupled device camera with Metamorph software.

Flutax-2 Competitive Binding Assay. Another tubulin polymerization assay was done to provide a more concentrated microtubule solution. In brief, 120 μL of 10 mg/mL tubulin, 80 mM PIPES, pH 6.9, 2 mM MgCl₂, 0.5 mM EGTA, 7.8% glycerol, 1 mM GTP were incubated in a microtiter plate, and the growth of microtubules at 37 °C was followed via optical density using BMG FLUOstar Omega microplate reader using the same settings as before. The concentration of polymerized tubulin was estimated from the curve. This tubulin was used in a competitive binding assay employing the fluorescent taxoid, flutax-2. Increasing concentrations of flutax-2 were added to microtubule solutions (final concentration of nearly 2.5 μM polymerized tubulin) in the presence or absence of lankacidin C (final concentration of 128 μM) to a final volume of 60 μL. Final concentrations of 80 mM PIPES, pH 6.9, 2 mM MgCl₂, 0.5 mM EGTA, 7.8% glycerol, 1 mM GTP were maintained in all the samples, and all the steps were performed at 37 °C to maintain the stability of microtubules. The samples were incubated at 37 °C for about 1 h and then centrifuged in Beckman Coulter Optima Max-Up Ultracentrifuge for 30 min at 50 000 rpm and 37 °C to separate microtubules. The supernatant was discarded, and the pellets were resuspended in 120 μL of 10 mM phosphate, 1% SDS buffer (pH 7.0). The fluorescence intensity of each sample was measured three times on 384-well Black OptiPlate microplate (PerkinElmer) by Envision 2103 multilabel plate reader (PerkinElmer), employing 485 nm excitation wavelength and 538 nm emission wavelength. The binding curve in the presence or absence of lankacidin C was drawn by GraphPad Prism, and binding constants were estimated.

Binding to Free Tubulin. Fluorescence Quenching Assay. Porcine brain tubulin (catalog no. T240-DX) was purchased from Cytoskeleton Inc. Fluorescence emission spectra were recorded on a PTI MODEL-MP1 spectrofluorometer using a 1 cm fluorescence cell for all measurements. The excitation wavelength was 295 nm, and the scan range was 310–450 nm. The genes for human βI, and αI-tubulin were purchased from DNA2.0 (Menlo Park, CA, USA). All reagents were purchased from Sigma-Aldrich Canada Ltd. (Oakville, Ontario, Canada) and Fisher Scientific Company (Ottawa, Ontario, Canada). Nickel-NTA resin was purchased from Qiagen Inc. (Toronto, Ontario, Canada).

In a 96-well microplate, equimolar mixtures of recombinant human tubulin αI-βI (prepared as described in the Supporting Information) or porcine cytoskeleton tubulin protein (purchased from Cytoskeleton Inc.; catalog no. T240-DX) and the buffer (10 mM sodium phosphate, 10 mM MgCl₂, 1 mM guanosine 5'-triphosphate (GTP), 0.5% DMSO, 250 mM sucrose, pH 7.0) were mixed to reach a final tubulin dimer concentration of 2 μM. GTP was added to the samples to a final concentration of 1 mM. The microplate was incubated on ice for 10 min. The calculated amounts of stock solution of the compounds in DMSO were added to the protein samples to obtain final ligand concentrations of 5, 10, 20, 40, 60, 80, and 100 μM. The control was

ligand-free, and the total sample volume was 100 μL . A glass bead was inserted into each well, and the microplate was covered with a protective film, sealed with a lid, and incubated for 30 min at 25 $^{\circ}\text{C}$. After that time, the microplate was transferred to a rotating platform and vigorously rotated for 1 h at room temperature. From each well, 80 μL of the samples and control were transferred to a 1 cm fluorescence cell. Fluorescence spectra were collected on a PTI MODEL-MP1 spectrofluorometer using 10 mm path length cell at 295 nm (excitation wavelength), and the scan range was 310–400 nm. Spectral data were collected using fluorescence software, and data analysis was performed using ORIGIN 6.1 software (OriginLab, Northampton, MA).

Determination of Kinetic Parameters. Data from the fluorescence quenching assays were used to determine the apparent binding constant of ligands to tubulin dimers by using the Stern–Volmer equation:

$$\frac{F_0 - F}{F} = K_a[L] \quad (3)$$

Here F_0 and F are the fluorescence intensities in the absence and in the presence of quencher, K_a is the formation constant of the donor–acceptor (quencher–fluorogen) complex, and $[L]$ is the concentration of the ligand added. Excitation and emission slits were set at 4 nm. All spectra were collected with samples having final optical densities (1 cm) of <0.3 at maximum absorbance of added ligand and were corrected for the inner filter effect according to the following equation:

$$F_{\text{corr}} = 10^{(A_{\text{ex}} + A_{\text{em}})/2} F_{\text{obs}} \quad (4)$$

where F_{corr} is the corrected fluorescence, F_{obs} is the measured fluorescence, A_{ex} is the absorption value at the excitation wavelength (295 nm), and A_{em} is the absorption value at the emission wavelength (336 nm). From the slope of the linear plot of $(F_0 - F)/F$ versus $[L]$, binding constant values were estimated. The results are expressed as mean values \pm SD ($n = 4$).

■ ASSOCIATED CONTENT

Supporting Information

The Supporting Information is available free of charge on the ACS Publications website at DOI: 10.1021/acs.jmedchem.6b01264.

Molecular formula strings (CSV)

^1H NMR spectra and HPLC chromatograms of lankacidin C and lankacidinol A and experimental procedures for the preparation of human αI and βI tubulin (PDF)

■ AUTHOR INFORMATION

Corresponding Author

*Phone: +20 100 830 8662. E-mail: atayoub@ualberta.ca.

Notes

The authors declare no competing financial interest.

■ ACKNOWLEDGMENTS

C.W.L. is funded by a NSERC Alexander Graham Bell Canada Graduate Scholarship. G.C. is funded by NSERC and Cancer Research Society. This research was partially supported by NSERC Discovery Grant to M.K. We deeply thank Dr. Manjeh Pasdar, University of Alberta, for allowing us to use her lab and equipment for the experimental part of the study.

■ ABBREVIATIONS USED

MM/PBSA, molecular mechanics/Poisson–Boltzmann surface area; DAPI, 4',6-diamidino-2-phenylindole; OD340, optical density at 340 nm; Pac, paclitaxel; LC, lankacidin C; Me, mebendazole; Tub, tubulin; EGTA, ethylene glycol-bis(β -

aminoethyl ether)- N,N,N',N' -tetraacetic acid; Flu, flutax; FI, fluorescence intensity; FBS, fetal bovine serum; DMEM, Dulbecco's modified Eagle medium

■ REFERENCES

- (1) Harada, S.; Higashide, E.; Fugono, T.; Kishi, T. Isolation and structures of T-2636 antibiotics. *Tetrahedron Lett.* **1969**, *10*, 2239–2244.
- (2) Harada, S.; Kishi, T.; Mizuno, K. Studies on T-2636 antibiotics. II. Isolation and chemical properties of T-2636 antibiotics. *J. Antibiot.* **1971**, *24*, 13–22.
- (3) Harada, S.; Tanayama, S.; Kishi, T. Studies on lankacidin-group (T-2636) antibiotics. 8. Metabolism of lankacidin C 14-propionate in rats and mice. *J. Antibiot.* **1973**, *26*, 658–668.
- (4) Harada, S.; Yamazaki, T.; Hatano, K.; Tsuchiya, K.; Kishi, T. Studies on lankacidin-group (T-2636) antibiotics. VII. Structure-activity relationships of lankacidin-group antibiotics. *J. Antibiot.* **1973**, *26*, 647–657.
- (5) Harada, S.; Kishi, T. Studies on lankacidin-group (T-2636) antibiotics. V. Chemical structures of lankacidin-group antibiotics. *1. Chem. Pharm. Bull.* **1974**, *22*, 99–108.
- (6) Tsuchiya, K.; Yamazaki, T.; Takeuchi, Y.; Oishi, T. Studies on T-2636 antibiotics. IV. In vitro and in vivo antibacterial activity of T-2636 antibiotics. *J. Antibiot.* **1971**, *24*, 29–41.
- (7) Ayoub, A. T.; Klobukowski, M.; Tuszynski, J. Similarity-based virtual screening for microtubule stabilizers reveals novel antimetastatic scaffold. *J. Mol. Graphics Modell.* **2013**, *44*, 188–196.
- (8) Ootsu, K.; Matsumoto, T. Effects of lankacidin group (T2636) antibiotics on the tumor growth and immune response against sheep erythrocytes in mice. *Gann* **1973**, *64*, 481–492.
- (9) Ootsu, K.; Matsumoto, T.; Harada, S.; Kishi, T. Antitumor and immunosuppressive activities of lankacidin-group antibiotics: structure-activity relationships. *Cancer Chemother. Rep.* **1975**, *59*, 919–928.
- (10) Kende, A. S.; Liu, K.; Kaldor, I.; Dorey, G.; Koch, K. Total synthesis of the macrolide antitumor antibiotic lankacidin C. *J. Am. Chem. Soc.* **1995**, *117*, 8258–8270.
- (11) Auerbach, T.; Mermershtain, I.; Davidovich, C.; Bashan, A.; Belousoff, M.; Wekselman, I.; Zimmerman, E.; Xiong, L.; Klepacki, D.; Arakawa, K.; Kinashi, H.; Mankin, A. S.; Yonath, A. The structure of ribosome-lankacidin complex reveals ribosomal sites for synergistic antibiotics. *Proc. Natl. Acad. Sci. U. S. A.* **2010**, *107*, 1983–1988.
- (12) Belousoff, M. J.; Shapira, T.; Bashan, A.; Zimmerman, E.; Rozenberg, H.; Arakawa, K.; Kinashi, H.; Yonath, A. Crystal structure of the synergistic antibiotic pair, lankamycin and lankacidin, in complex with the large ribosomal subunit. *Proc. Natl. Acad. Sci. U. S. A.* **2011**, *108*, 2717–2722.
- (13) Risinger, A. L.; Mooberry, S. L. Cellular studies reveal mechanistic differences between tacalolonide A and paclitaxel. *Cell Cycle* **2011**, *10*, 2162–2171.
- (14) Shelanski, M. L.; Gaskin, F.; Cantor, C. R. Microtubule assembly in the absence of added nucleotides. *Proc. Natl. Acad. Sci. U. S. A.* **1973**, *70*, 765–768.
- (15) Lee, J. C.; Timasheff, S. N. In vitro reconstitution of calf brain microtubules: effects of solution variables. *Biochemistry* **1977**, *16*, 1754–1764.
- (16) Buey, R. M.; Barasoain, I.; Jackson, E.; Meyer, A.; Giannakakou, P.; Paterson, I.; Mooberry, S.; Andreu, J. M.; Diaz, J. F. Microtubule interactions with chemically diverse stabilizing agents: thermodynamics of binding to the paclitaxel site predicts cytotoxicity. *Chem. Biol.* **2005**, *12*, 1269–79.
- (17) Hornak, V.; Abel, R.; Okur, A.; Strockbine, B.; Roitberg, A.; Simmerling, C. Comparison of multiple AMBER force fields and development of improved protein backbone parameters. *Proteins: Struct., Funct., Bioinf.* **2006**, *65*, 712–725.
- (18) Meagher, K. L.; Redman, L. T.; Carlson, H. A. Development of polyphosphate parameters for use with the AMBER force field. *J. Comput. Chem.* **2003**, *24*, 1016–1025.

(19) Wang, J.; Wolf, R. M.; Caldwell, J. W.; Kollman, P. A.; Case, D. A. Development and testing of a general amber force field. *J. Comput. Chem.* **2004**, *25*, 1157–74.

(20) Case, D. et al. *AMBER 12*; University of California, San Francisco, 2012.

(21) Kinashi, H.; Mori, E.; Hatani, A.; Nimi, O. Isolation and characterization of linear plasmids from lankacidin-producing *Streptomyces* species. *J. Antibiot.* **1994**, *47*, 1447–1455.

(22) Arakawa, K.; Sugino, F.; Kodama, K.; Ishii, T.; Kinashi, H. Cyclization mechanism for the synthesis of macrocyclic antibiotic lankacidin in *Streptomyces rochei*. *Chem. Biol.* **2005**, *12*, 249–256.

(23) Chan, G. K. T.; Jablonski, S. A.; Starr, D. A.; Goldberg, M. L.; Yen, T. J. Human ZW10 and ROD are mitotic checkpoint proteins that bind to kinetochores. *Nat. Cell Biol.* **2000**, *2*, 944–947.